THE JOURNAL OF BIOLOGICAL CHEMISTRY VOL. 284, NO. 15, pp. 9781–9787, April 10, 2009

Synaptotagmin 2 Couples Mucin Granule Exocytosis to Ca^{2+} Signaling from Endoplasmic Reticulum*[S]

Received for publication, October 10, 2008, and in revised form, January 16, 2009 Published, JBC Papers in Press, February 10, 2009, DOI 10.1074/jbc.M807849200

Michael J. Tuvim[‡1], Andrea Rossi Mospan[§1], Kimberlie A. Burns[¶], Michael Chua[§], Peter J. Mohler[‖], Ernestina Melicoff[‡], Roberto Adachi[‡], Zoulikha Ammar-Aouchiche[‡], C. William Davis[§¶], and Burton F. Dickey[‡2]

From the [‡]Department of Pulmonary Medicine, University of Texas M.D. Anderson Cancer Center, Houston, Texas 77030, the [§]Department of Cell and Molecular Physiology and [¶]Cystic Fibrosis/Pulmonary Research and Treatment Center, University of North Carolina, Chapel Hill, North Carolina 27599, and the [‖]Department of Internal Medicine, Division of Cardiology, University of Iowa, Iowa City, Iowa 52242

Synaptotagmin 2 (Syt2) functions as a low affinity, fast exocytic Ca^{2+} sensor in neurons, where it is activated by Ca^{2+} influx through voltage-gated channels. Targeted insertion of *lacZ* into the mouse *syt2* locus reveals expression in mucin-secreting goblet cells of the airways. In these cells, rapid Ca^{2+} entry from the extracellular medium does not contribute significantly to stimulated secretion (Davis, C. W., and Dickey, B. F. (2008) *Annu. Rev. Physiol.* 70, 487–512). Nonetheless, $Syt2^{-/-}$ mice show a severe defect in acute agonist-stimulated airway mucin secretion, and $Syt2^{+/-}$ mice show a partial defect. In contrast to Munc13-$2^{-/-}$ mice (Zhu, Y., Ehre, C., Abdullah, L. H., Sheehan, J. K., Roy, M., Evans, C. M., Dickey, B. F., and Davis, C. W. (2008) *J. Physiol.* (*Lond.*) 586, 1977–1992), $Syt2^{-/-}$ mice show no spontaneous mucin accumulation, consistent with the inhibitory action of Syt2 at resting cytoplasmic Ca^{2+} in neurons. In human airway goblet cells, inositol trisphosphate receptors are found in rough endoplasmic reticulum that closely invests apical mucin granules, consistent with the known dependence of exocytic Ca^{2+} signaling on intracellular stores in these cells. Hence, Syt2 can serve as an exocytic sensor for diverse Ca^{2+} signaling systems, and its levels are limiting for stimulated secretory function in airway goblet cells.

Mucin secretion in the airways of the lungs is crucial for clearance of inhaled particulates and pathogens (1). However, mucin hypersecretion is a leading cause of mortality in common diseases such as asthma and cystic fibrosis (2). Thus, tight control of mucin secretion is critical for lung homeostasis. Airway mucin secretion is stimulated by triphosphate nucleotides secreted into the extracellular lumenal liquid layer (3). These bind to epithelial apical $P2Y_2$ receptors that activate G_q, which in turn activates phospholipase $C\beta_1$ generating the intracellular second messengers diacylglycerol and inositol trisphosphate (IP_3).[3] Diacylglycerol directly induces mucin granule exocytosis by activating the priming protein Munc13-2 (4), and indirectly regulates exocytosis by activating protein kinase Cϵ (5). IP_3 induces the release of Ca^{2+} from intracellular stores, resulting in a rise in cytoplasmic Ca^{2+} that rapidly triggers mucin granule exocytosis (6–9). However, the precise mechanism by which a rise in cytoplasmic Ca^{2+} is coupled to exocytosis in goblet cells is not known.

Synaptotagmins (Syts) are a family of structurally related proteins of which several are known to mediate Ca^{2+}-dependent exocytosis. Syts are composed of a short intravesicular amino terminus, a transmembrane domain, a variable linker region, and two conserved C_2 domains near the carboxyl terminus (10, 11). There are at least 15 Syt family members encoded in mammalian genomes. Of these, eight (Syt1–3, -5–7, -9, and -10) display Ca^{2+}-dependent phospholipid binding that is thought to be essential for Ca^{2+}-dependent exocytosis (12–16). A subset of three of these (Syt1, -2, and -9) binds Ca^{2+} with low affinity ($\sim 10\ \mu M$) and high cooperativity ($n = 5$) and functions as fast, synchronous Ca^{2+} sensors in neurons (16). Syt1 mediates synchronous synaptic vesicle release in forebrain neurons, and also mediates rapid exocytosis in adrenal chromaffin cells (15, 16). Like neurons, chromaffin cells express voltage-gated Ca^{2+} channels activated by neurotransmitter-induced depolarization. Syt2 mediates synchronous synaptic vesicle release in hindbrain neurons and at the neuromuscular junction (14, 17), but it has not been previously known to function outside the nervous system. Syt9 mediates synchronous synaptic vesicle release from limbic and striatal neurons (16), and it also functions in dense core granule release from the PC12 chromaffin cell line (18–20) and insulin release from pancreatic islet cells (21, 22). In islet cells, membrane depolarization and opening of voltage-gated Ca^{2+} channels is induced by closure of K_{ATP} channels when blood glucose is elevated. To our knowledge, there has been no analysis of the function of a low Ca^{2+} affinity, fast Syt in a nonexcitable cell (*i.e.* a cell not expressing voltage-gated Ca^{2+} channels).

* This work was supported, in whole or in part, by National Institutes of Health Grants HL072984, HL094848, CA105352, CA016672, and HL063756. This work was also supported by grants from the North American Cystic Fibrosis Foundation and American Heart Association.

[S] The on-line version of this article (available at http://www.jbc.org) contains supplemental Figs. S1 and S2.

[1] Both authors contributed equally to this work.

[2] To whom correspondence should be addressed: Pulmonary Medicine, Unit 1462, M. D. Anderson Cancer Center, 1515 Holcombe Blvd., Houston, TX 77030. Tel.: 713-563-4253; Fax: 713-794-4922; E-mail: bdickey@mdanderson.org.

[3] The abbreviations used are: IP_3, inositol trisphosphate; IP_3-R, inositol trisphosphate receptor; Syt2, synaptotagmin 2; CCSP, Clara cell secretory protein; PDI, protein disulfide isomerase; MUC5AC, human mucin 5AC; X-gal, 5-bromo-4-chloro-3-indolyl-β-D-galactopyranoside; PAFS, periodic acid-fluorescent Schiff; WT, wild type; ER, endoplasmic reticulum; PBS, phosphate-buffered saline; IL, interleukin.

EXPERIMENTAL PROCEDURES

Materials—Affinity-purified pan-IP_3-R (23) and Rab3D antibodies (24) and ankyrin-B (25) and Clara cell secretory protein (CCSP) antibodies (24) have been described. Rabbit antibodies against mature MUC5AC (26) were from John Sheehan (University of North Carolina, Chapel Hill), and against Syt2 (A320) (14) were from Thomas Sudhof (University of Texas Southwestern Medical Center). We purchased mouse monoclonal antibodies against protein disulfide isomerase (PDI) (S34200; Molecular Probes), immature MUC5AC (MAB201; Chemicon), and acetylated tubulin (T6793; Sigma); goat antibodies against β-galactosidase (4600-1409; Biogenesis); fluorescein isothiocyanate-conjugated goat anti-mouse IgG, and Texas Red-conjugated goat anti-rabbit IgG secondary antibodies (Jackson ImmunoResearch); bovine serum albumin (A7906; Sigma); VectaShield mounting medium (Vector Laboratories); Superfrost/Plus microscope slides and coverglasses (Fisher); Liquid Blocker Super Pap Pens (Daido Sangyo); and Polybed resin (Polysciences).

Mice—Generation of a *syt2* null allele was described previously (14). Mice carrying this allele were backcrossed for 11 generations onto a C57BL/6 background and studied at the M. D. Anderson Cancer Center in accordance with its Institutional Animal Care and Use Committee. Mice with an ankyrin-B null allele have been carried on a C57BL/6 background (27) and were studied at the University of North Carolina, Chapel Hill, in accordance with its Institutional Animal Care and Use Committee. Experimental animals and wild-type (WT) littermate controls were obtained from heterozygous crosses. For immunoblot and histochemical analyses, mice were euthanized by CO_2 asphyxiation, and their lungs were harvested.

Human Tissue—Human lung tissue was obtained from normal and cystic fibrosis patients according to the guidelines of the Committee on the Protection of the Rights of Human Subjects of the University of North Carolina, Chapel Hill. The lung tissue was either immediately frozen in OCT embedding medium (Sakura) on dry ice, fixed in 10% neutral buffered formalin, or fixed in buffered aldehyde (2% glutaraldehyde and 2% paraformaldehyde).

Immunoblots—Lung tissue was homogenized in PBS containing a mixture of protease inhibitors in DMSO (P8340; Sigma), diluted 1:1,000, and consisted of 4-(2-aminoethyl)benzenesulfonyl fluoride, *N*-(trans-epoxysuccinyl)-L-leucyl-amido-(4-guanidino)butylamide, pepstatin A, bestatin, leupeptin, and aprotinin. Protein concentrations were determined by bicinchoninic acid assay (Pierce); equal amounts of protein were loaded for SDS-PAGE, and the resolved proteins were electrotransferred to nitrocellulose. Blots were probed with antibodies against Syt2 to measure its expression in lungs (14) or against IP_3-R, ankyrin-B, and PDI (23) to determine antibody specificity in lung tissue, all as described.

Histochemistry of Mouse Tissues—For β-galactosidase staining, lungs from adult Syt2 heterozygous mutant mice and WT controls were fixed in 0.2% glutaraldehyde, incubated with X-gal, dehydrated, embedded in paraffin, sectioned, deparaffinized, rehydrated, and counterstained with treosin as described (14) or co-stained immunohistochemically for CCSP as described (24) and then examined by bright field microscopy. For immunocolocalization of β-galactosidase with cell lineage markers, tissues from neonatal homozygous mutant mice and WT controls were fixed with 4% paraformaldehyde, embedded in paraffin, sectioned, deparaffinized, and labeled with antibodies against β-galactosidase, CCSP, and acetylated tubulin as described (28) and then examined by fluorescence microscopy.

Mucin Secretion in Mouse Airways—The apical secretory cells of the intrapulmonary airways of mice and the small distal airways of humans lack histochemically apparent mucin under base-line healthy conditions, although intracellular mucin can be demonstrated using sensitive immunohistochemical techniques (4, 24, 29, 30). Under base-line conditions, these airway secretory cells are often termed Clara cells (24). When production of gel-forming polymeric mucins is increased by allergic or infectious inflammation, intracellular mucin becomes histochemically apparent under the rubric "mucous metaplasia," and these airway secretory cells are generally termed goblet or mucous cells although they continue to express the Clara cell marker CCSP (24, 30). The secretory cells of the large airways of humans often contain histochemically apparent mucin even under base-line conditions (30). To induce mucous metaplasia in mouse airways for the measurement of mucin secretion, post-natal day 16 pups and their mothers were exposed for 60 min to an aerosolized solution of 0.225 mg/ml human IL-13 (Wyeth) in PBS generated by an AeroMist CA-209 nebulizer (CIS-US) driven by 10 liters/min of 5% CO_2 in air to increase ventilation, with a calculated deposition of 0.5 μg of IL-13 per mouse. Three days later, mice were exposed to a 100 mM aerosol of ATP in PBS for 5 min to induce mucin secretion (24), then euthanized by CO_2 asphyxiation, and their lungs harvested. Mucous metaplasia was also induced in adult heterozygous mice by ovalbumin sensitization and challenge as described (24), and mucin secretion was stimulated with aerosolized ATP as for the pups. Intracellular epithelial mucin was measured before and after ATP stimulation by staining with periodic acid-fluorescent Schiff's (PAFS) reagent, as described (24). In brief, lungs were fixed with 4% paraformaldehyde in 0.1 M phosphate buffer (pH 7.2) infused through a tracheal cannula at 21 °C, then removed from the thoracic cavity, and further fixed overnight at 4 °C, embedded in paraffin, sectioned, and stained for fluorescence microscopy. Data are presented as the volume of intracellular mucin per surface area of the basement membrane, which is derived as the ratio of epithelial area with red fluorescence staining to total epithelial area divided by a boundary length measurement that is a product of the total epithelial area, the basement membrane length, and the geometric constant $4/\pi$ to yield an idealized cylindrical cell (24).

Confocal Microscopy of Human Tissues—For IP_3-R immunohistochemistry, formalin-fixed human lung tissue was dehydrated and embedded in paraffin; sections were cut at 5 μm, deparaffinized, and rehydrated. For the other antibodies, frozen sections were fixed in cold 100% methanol for 10 min, washed with PBS, blocked with 3% bovine serum albumin in PBS for 2 h at 21 °C, and incubated with primary antibody overnight at 4 °C and then the appropriate secondary antibody for 1 h at 21 °C, both diluted in blocking solution. Immunofluorescence was

visualized using a Leica SP2 or Zeiss 510 laser scanning confocal microscope, and oil immersion 40× Apochromat and 63× plan-Apochromat objectives (1.25 and 1.4 NA, respectively), with excitation from a 488-nm argon and a 568-nm krypton laser (Leica SP2) or a 543-nm HeNe laser (Zeiss 510). Photomultiplier gains and offsets for the two fluorescence channels were adjusted to minimize cross-talk, and differential interference microscopy was used in a third channel for general morphology. Simple PCI (Compix) and Zeiss 510 imaging software were used for image analysis and quantitation. For each experiment, the immunostaining procedure was repeated a minimum of three times using tissue from at least three subjects, at least one of which came from a patient with non-cystic fibrosis. The images and protein distributions presented are fully representative, and there were no apparent differences in the described parameters between cystic fibrosis and non-cystic fibrosis tissues.

Electron Microscopy—Aldehyde-fixed human lung tissue was post-fixed in 1% OsO_4 for 1 h at 4 °C, dehydrated, immersed two times in propylene oxide for 20 min, then infiltrated with Epon resin, and polymerized. Sections of 90 nm were cut onto copper grids, stained with uranyl acetate followed by lead citrate, and viewed with a Zeiss EM900 transmission electron microscope.

RESULTS

Syt2 Expression in Airway Epithelium—We found Syt2 in the lungs of WT but not null mice by immunoblot analysis (Fig. 1*A*), raising the possibility that Syt2 serves as an exocytic Ca^{2+} sensor in secretory epithelial cells. *Syt2* null mice had been generated by knocking IRES-*lacZ* with a nuclear localization signal into the *syt2* locus under the transcriptional control of the native *Syt2* regulatory elements (14). We found X-gal staining in the nuclei of non-ciliated cells of the bronchial epithelium of neonatal (Fig. 1*B*) and adult (data not shown) heterozygous mice. Localization of Syt2 to airway secretory (Clara) cells was confirmed by colocalization of X-gal$^+$ nuclei within CCSP$^+$ cells (24) (Fig. 1*C*). By dual immunofluorescence colocalization, β-galactosidase was detected in the nuclei and cytoplasm of virtually all CCSP-labeled airway epithelial secretory cells (Fig. 1*D* and supplemental Fig. 1) but no acetylated tubulin-labeled ciliated cells (Fig. 1*E*). Despite localizing *Syt2* expression to airway secretory cells through analysis of *lacZ* expression, we were unable to detect Syt2 immunohistochemically in the airways of WT mice even though it can be readily detected in neurons (14, 17). This suggests that the level of Syt2 protein in airway secretory cells is less than in neurons.

Mucin Secretory Function in Syt2 Null Mice—We analyzed airway secretory cell function by measuring the release of intracellular mucin after stimulation with the strong secretagogue ATP. Because the small amount of intracellular mucin present within the secretory cells of mouse airways under base-line uninflamed conditions is not visible histochemically (see "Experimental Procedures"), we first increased polymeric gel-forming mucin production with IL-13 (*i.e.* induced mucous metaplasia) (24). *syt2* null mice have severe motor dysfunction and die at the time of weaning (P19–P24) (14), so post-natal day 16 pups of mixed genotypes and their heterozygous mothers were exposed to an IL-13 aerosol. This led to robust mucin gene expression in all genotypes, apparent as abundant intracellular PAFS staining 3 days after IL-13 exposure (Fig. 2*A*, *top row*), compared with faint patchy PAFS staining in mice of all genotypes not exposed to IL-13 (data not shown). We then stimulated mucin secretion by activating $P2Y_2$ receptors with an ATP aerosol. The airway epithelial cells of WT pups secreted most of their PAFS-positive intracellular mucin within 5 min. In contrast, the epithelial cells of homozygous null pups showed a severe mucin secretory defect, and those of heterozygous pups showed an intermediate phenotype (Fig. 2). The heterozygous mothers exposed to the IL-13 aerosol showed a similar mucin secretory defect in response to the ATP aerosol (data not shown), and heterozygous adult mice of both sexes with mucous metaplasia induced by ovalbumin sensitization and challenge also showed a comparable secretory defect (Fig. 3).

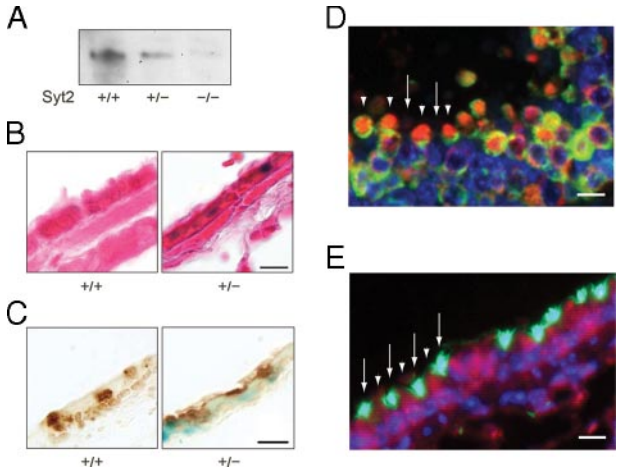

FIGURE 1. **Syt2 is expressed in airway secretory (Clara) cells.** *A,* Western-blotted lung homogenates from WT (+/+), heterozygous (+/−), and null (−/−) mutant mice were probed with rabbit polyclonal antibodies against Syt2. A single band was observed in WT and heterozygous mouse lung tissue at ~65 kDa. *B,* bronchial airways of WT and heterozygous mutant mice with *lacZ* knocked into the *syt2* locus were stained with X-gal (*blue*) and then counterstained with treosin (*red*). Blue staining is observed only in heterozygous mice in cells that do not contain ciliated tufts. *Scale bar* in all tissue sections = 10 μm. *C,* bronchial airways of WT and heterozygous mutant mice were stained with X-gal (*blue*) and then immunostained with rabbit polyclonal antibodies against mouse CCSP developed with diaminobenzidine (*brown*). Blue staining is observed in association with brown-stained Clara cells. *D,* bronchial airways of null mice were labeled with antibodies against β-galactosidase (*red*) and CCSP (*green*), and nuclei were labeled with 4′,6-diamidino-2-phenylindole (*blue*). Both *red* and *green* labeling are observed in Clara cells (*arrowheads*), alternating with ciliated cells that are not labeled with either antibody (*arrows*). Control WT mice show no red labeling (supplemental Fig. 1). *E,* bronchial airways of null mice were labeled with antibodies against β-galactosidase (*red*) or acetylated tubulin (*green*), and nuclei were labeled with 4′,6-diamidino-2-phenylindole (*blue*). *Red labeling* is observed in Clara cells that are not labeled with acetylated tubulin antibodies (*arrowheads*), whereas green labeling is observed in ciliated cells that are not labeled with β-galactosidase antibodies (*arrows*).

Proximity of ER to Mucin Secretory Granules—ATP-stimulated elevations in cytoplasmic Ca^{2+} in airway goblet cells are due primarily to IP_3-mediated release from intracellular stores (3, 7, 9). IP_3 typically acts on Ca^{2+}-release channels in the ER in non-muscle cells, so we examined the localization of ER in cells of human airway epithelium using antibodies to PDI whose specificity in lung tissue was verified by immunoblot analysis (supplemental Fig. 2*A*). Immunostaining of lung sections showed ER distributed around the nuclei of basal, ciliated, and

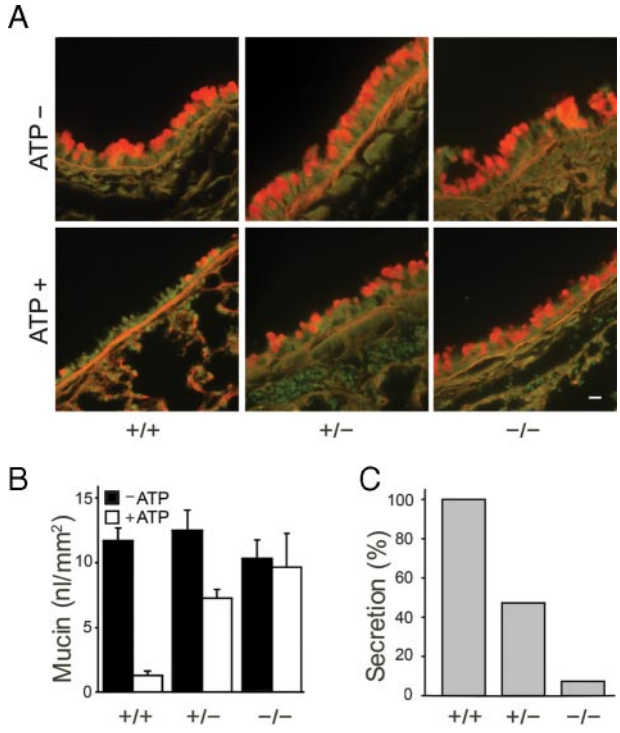

FIGURE 2. **Syt2 mediates stimulated mucin secretion.** *A,* bronchial airways of WT, heterozygous, and homozygous mutant P19 mice that had had been exposed 3 days earlier to aerosolized IL-13 to induce mucous metaplasia (*top row*), then exposed to aerosolized ATP to induce mucin secretion (*bottom row*), were stained for intracellular mucin with PAFS (*orange*). *Scale bar,* 10 μm. *B,* intracellular mucin content of bronchial airways from three experiments such as that in Fig. 2*A*, which included at least three pups of each genotype and five sections from each airway, was measured and analyzed. *C,* data from *B* are replotted as the percentage of intracellular mucin released for each genotype relative to WT.

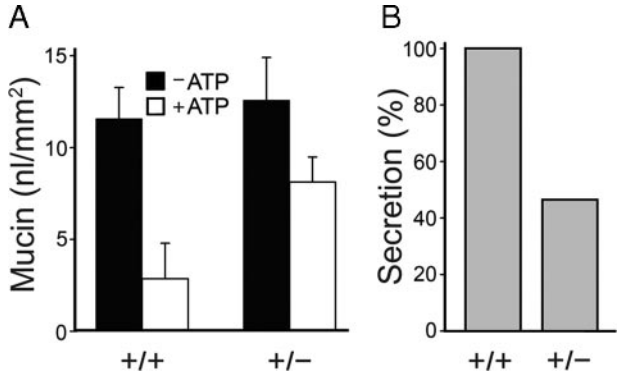

FIGURE 3. **Airway mucin secretion is impaired in heterozygous *Syt2* mutant adult mice.** *A,* mucous metaplasia was induced in the airways of WT and heterozygous adult mice of both sexes by intraperitoneal sensitization and aerosol challenge with ovalbumin. Three days later, secretion was stimulated by exposure to aerosolized ATP, and retained intracellular mucin was measured by PAFS staining as in Fig. 2. There was no difference in intracellular mucin content between heterozygous and WT mice in the absence of mucous metaplasia (~1 nl/mm^2, not shown) or in mice with mucous metaplasia prior to stimulation with the ATP aerosol (~12 nl/mm^2, *black bars*). However, heterozygous mice released only half as much mucin as WT mice after ATP stimulation (*white bars*). Shown are the results of a representative experiment that was performed three times with similar results. *B,* data from *A* are replotted as the percentage of intracellular mucin released for each genotype relative to WT.

goblet cells and throughout the cytoplasm of goblet cells apical to the nuclei (Fig. 4*A*). The heavy staining of goblet cells for PDI is consistent with the demands of synthesizing disulfide-linked polymeric mucins (31). Ca^{2+} is heavily buffered in the cytoplasm, so changes in concentration are highly localized. Because Syt proteins are localized on the cytoplasmic surface of secretory vesicles (3), we examined the proximity of ER to mucin granules in goblet cells using confocal microscopy and antibodies against mature MUC5AC (matMUC5AC), the predominant secreted polymeric mucin of human airway epithelium (2). The PDI-positive ER apical to the nuclei of goblet cells surrounded matMUC5AC-positive mucin granules with little overlap of the two signals in the scattergram generated from the merged images (Fig. 4*A*).

ER in Goblet Cells Is Predominantly Rough ER—Airway goblet cells specialize in synthesis, storage, and secretion of polymeric mucins, so they could be expected to contain predominantly rough ER. To identify rough ER, human lung sections were labeled with antibodies to the immature, nonglycosylated form of MUC5AC (immatMUC5AC) (31). Confocal microscopy showed extensive colocalization of immatMUC5AC and PDI (Fig. 4*B*). By electron microscopy, the apical ER was seen to closely invest mucin granules, and confirmed to be predominantly rough ER (Fig. 4*C* and Fig. 6*A*). Golgi cisternae (Fig. 4*E*) and mitochondria (Fig. 6*A*) were interspersed among the ER and granules, similar to what we have observed in mouse airways (24).

Localization of IP3-R to ER Adjacent to Mucin Granules—IP_3-Rs have generally been localized to ER in secretory cells, but they have also been reported on secretory granules and plasma membrane (32–34). Human lung sections probed with a pan-IP_3-R antibody that is highly specific in lung tissue (supplemental Fig. 2*B*) showed a broad distribution of immunoreactivity in basal, goblet, and ciliated cells (Fig. 5*A*). In goblet cells, IP_3-R colocalized with the ER marker PDI (Fig. 5*A*), as expected. Presumably, membrane-localized IP_3-R appears to colocalize with lumenal PDI because of the sub-microscopic nature of the ER. Because mucin secretory granules are much larger (~0.5–1 μm), it was necessary to determine whether a granule surface marker would also appear to colocalize with matMUC5AC before testing whether IP_3-R is expressed on granule membranes. We found that Rab3D, a small GTPase implicated in regulated exocytosis that resides on the surface of secretory granules (24), has a distribution that correlated closely with that of matMUC5AC (Fig. 5*B*), indicating that granule lumenal and membrane proteins are indistinguishable under the optical conditions of these experiments. Finally, we found that IP_3-R and matMUC5AC resolve independently in co-stained images (Fig. 5*C*), indicating they populate distinct organelles. Hence, these data suggest that Ca^{2+} is released predominantly from the ER. Notably, the ER distributes to the vicinity of the apical membrane (Fig. 6*A*), positioned to provide Ca^{2+} locally to activate granules near exocytic docking sites.

DISCUSSION

Syt2 as the Major Stimulated Exocytic Ca^{2+} Sensor in Airway Goblet Cells—Our results indicate that Syt2 mediates >90% of acute mucin secretion in response to extracellular signals in airway goblet cells. Syt2 is one of three low affinity Ca^{2+} sensors that trigger fast synaptic vesicle release in neurons, together with Syt1 and Syt9 (16, 17). Of these, Syt2 is the fastest and is

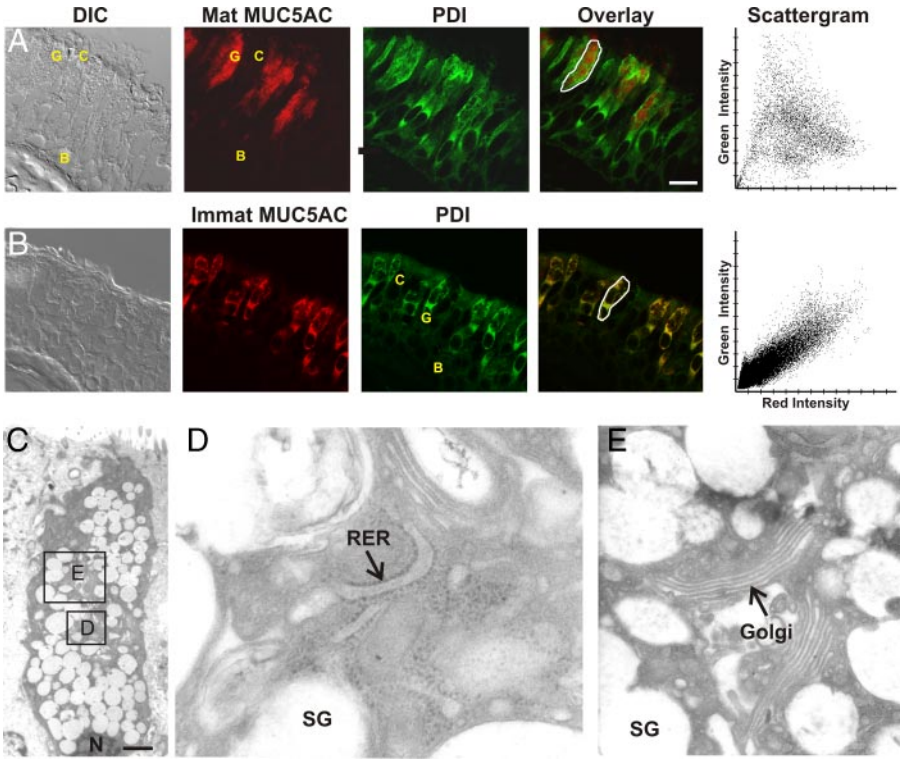

FIGURE 4. **ER apical to the nucleus of airway secretory cells is closely apposed to mucin secretory granules.** *A,* frozen human lung section imaged by differential interference contrast (*DIC*) microscopy (*left*) and labeled with antibodies against the secretory granule glycoprotein mature MUC5AC (*red*) and the lumenal ER resident protein PDI (*green*). An *overlay* image and a *scattergram* of the outlined goblet cell indicating the relative intensity of *red* and *green* labels for each pixel show a lack of colocalization of the two antibodies. Basal (*B*), ciliated (*C*), and goblet (*G*) cells are marked. *Scale bar*, 16 μm. *B,* ER in airway goblet cells is predominantly rough ER. A frozen human lung section labeled with antibodies against the newly synthesized cargo protein immature (nonglycosylated) MUC5AC (*red*) that labels only rough ER and antibodies against PDI (*green*) that labels both smooth and rough ER (31) shows a high degree of colocalization in the overlay image and scattergram. Scale identical to *A*. *C,* electron micrograph of a goblet cell from normal human lung, with the nucleus (*N*) marked. *Scale bar*, 2.5 μm. *D,* higher magnification of the area indicated in *C*, with rough ER (*RER*) and a mucin secretory granule (*SG*) marked. *E,* neighboring area from *C* at the same magnification, with Golgi apparatus (*Golgi*) and a mucin secretory granule (*SG*) marked.

expressed at synapses specialized for precise responses such as the calyx of Held (17). It is striking that Syt2 also serves as an exocytic Ca^{2+} sensor in goblet cells where the kinetics of stimulated exocytosis are measured in hundreds of milliseconds (35, 36) rather than the <2-ms time course of synchronous evoked synaptic vesicle release (10, 37). In goblet cells, the low affinity and high cooperativity of Ca^{2+} binding by Syt2 might ensure primarily the fidelity rather than the speed of signaling, in view of the danger of airway obstruction from excessive acute mucin release. For example, in death from asthma, asphyxiation occurs because of widespread plugging of airways with mucus (2). Similarly, airway liquid volume is tightly regulated by purinergic signaling with serious consequences to dysregulation in diseases such as cystic fibrosis (1).

Limitation of Goblet Cell Secretory Function by Syt2 Expression—Another striking finding of our studies is that acute airway mucin secretion in response to extracellular signals is reduced by ~50% in heterozygous null mice. The dependence of regulated exocytosis on Syt2 levels in goblet cells (Figs. 2 and 3) but not neurons (14, 17) could reflect a lower level of expression in goblet cells, differences in accessory proteins, or differences in physical properties of the systems. One such latter possibility is the greater size of mucin granules (~500 nm diameter) relative to synaptic vesicles (~40 nm diameter) if Syt2 is distributed over the granule surface, and the cooperation of several SNARE-Syt complexes is required for membrane fusion, as suggested (10, 11, 38). In addition, a relatively low level of expression of Syt2 in goblet cells is indicated by our inability to detect Syt2 immunohistochemically in the airway, although we are readily able to detect it in neurons (14, 17) and mast cells.[4] Because Syt2 inhibits exocytosis when not fully liganded by Ca^{2+} (14, 17, 39, 40), a low level of Syt2 expression in airway goblet cells could have adaptive value by allowing base-line mucin secretion through attenuation of this inhibitory function at resting cytoplasmic Ca^{2+} concentration (see comparison with Munc13-2 null mice, below). In contrast, spontaneous secretion by neurons reduces the fidelity of neural signaling, and spontaneous secretion by mast cells would induce inflammation, so there could be adaptive value to tightly constraining unstimulated release from these cell types through high levels of Syt2 expression.

Coupling of Syt2 to Intracellular Ca^{2+} Stores—Despite the different mechanisms of Ca^{2+} elevation in goblet cells compared with neurons and other excitable cells, the Ca^{2+} dependence (EC_{50} = 5.5 μM) of Syt2 binding to phospholipids (41) fits well with IP_3-induced Ca^{2+} concentrations (10 μM) in the vicinity of the exocytic machinery we have estimated in goblet cells (6). IP_3-Rs localized in the ER of goblet cells are in close apposition to secretory granules that presumably contain the Ca^{2+} sensor Syt2 (Figs. 4–6) (42), consistent with prior evidence in goblet cells for a proximity of Ca^{2+} channels to the exocytic Ca^{2+} sensor <50 nm using the fast Ca^{2+} buffer 1,2-bis(2-aminophenoxy)ethane-*N*,*N*,*N*′,*N*′-tetraacetic acid (6). These findings, together with the presence of mitochondria (Fig. 6*A*) (24, 43) that have well established roles in Ca^{2+} homeostasis (33, 44), indicate that the machinery for generating and responding to an exocytic Ca^{2+} signal are colocalized in the apical pole of goblet cells, where extracellular signals are sensed and mucins secreted (Fig. 6). The reliance of airway secretory cells on intracellular Ca^{2+} stores may reflect the instability of Ca^{2+} concentrations in airway lining fluid (45, 46), which is directly exposed to the external environment and to large amounts of Ca^{2+} released as counterions during the decondensation of highly anionic secreted mucins

[4] E. Melicoff and R. Adachi, unpublished data.

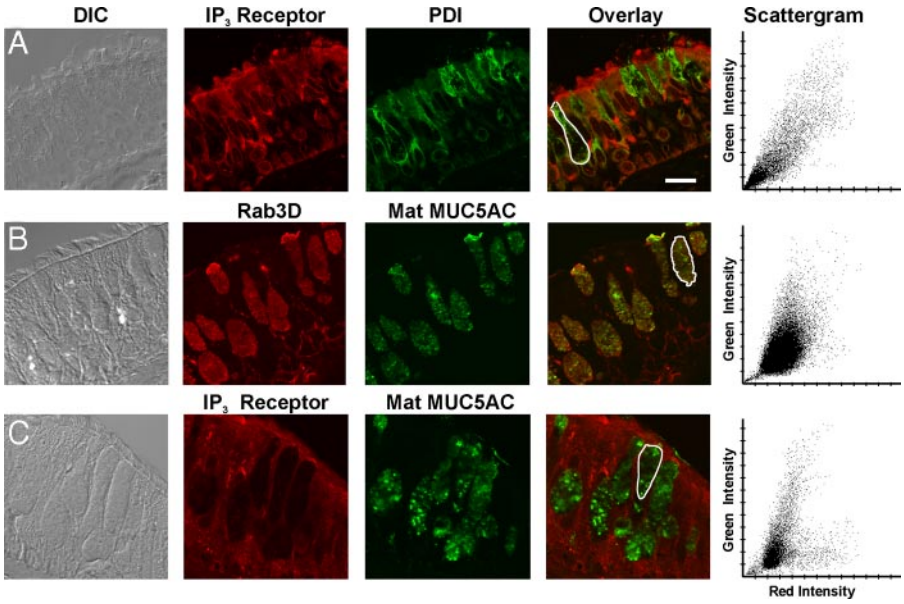

FIGURE 5. **IP_3-Rs are concentrated in apical ER adjacent to mucin secretory granules but not on granule membranes.** *A,* frozen human lung section labeled with antibodies against IP_3-R (*red*) and PDI (*green*), with the *scattergram* showing colocalization in the goblet cell outlined in the *overlay* image. *Scale bar,* 16 μm. *DIC,* differential interference contrast. *B,* mucin granule membrane and lumenal proteins are not resolved under the optical conditions of our experiments. Paraffin-embedded human lung section labeled with antibodies against the secretory granule surface protein Rab3D (*red*) and antibodies against the secretory granule lumenal protein mature MUC5AC (*green*), with the scattergram showing colocalization in the cell outlined in the overlay image. *C,* IP3-R are not detected on mucin granules. Paraffin-embedded human lung section labeled with antibodies against IP_3-R (*red*) and mature MUC5AC (*green*) is shown, with the scattergram showing a lack of colocalization in the cell outlined in the overlay image (note the splaying of two clearly separated populations of points to their respective axes).

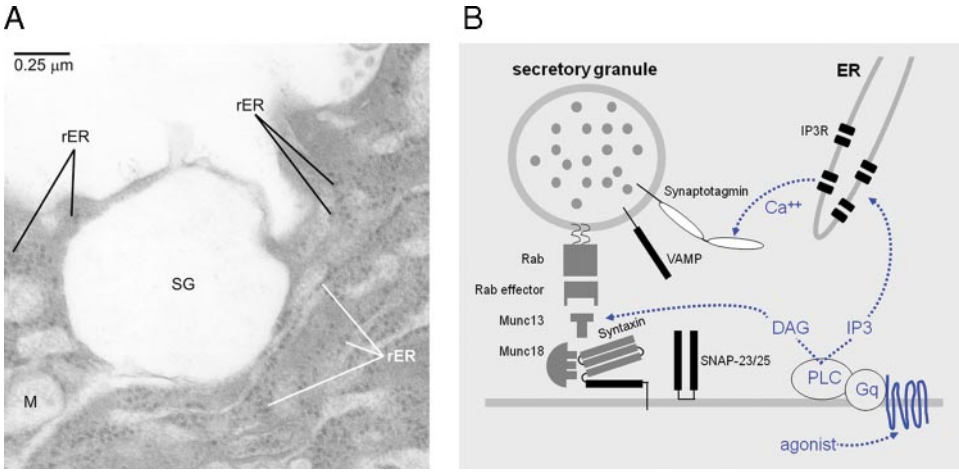

FIGURE 6. **Juxtaposition of apical endoplasmic reticulum and mucin secretory granules.** *A,* electron micrograph of the apical membrane region of a goblet cell, showing the juxtaposition of a mucin secretory granule (*SG*) and rough endoplasmic reticulum (*rER*). This human lung specimen was fixed ~24 h after harvest for transplantation, and hence fixation is not optimal and internal membrane structures are not well preserved. Nonetheless, the arrays of ribosomes reveal the rough ER and show the intimate relationships between the plasma membrane, granule, rough ER, and mitochondria (*M*). *B,* pathway for activation of regulated secretion in airway goblet cells. Extracellular ligands in the airway surface liquid layer (*bottom*) bind to heptahelical receptors in the apical membrane that activate G_q and phospholipase (*PLC*) β1, generating the second messengers diacylglycerol (*DAG*) and inositol trisphosphate (IP_3). Diacylglycerol activates the exocytic priming protein Munc13-2 (*dotted blue arrow, left fork*) and the exocytic regulator protein kinase Cϵ (data not shown). IP_3 induces the release of Ca^{2+} from endoplasmic reticulum (*ER*) in the vicinity of mucin-containing secretory granules, activating Syt2 on the surface of secretory granules (*dotted blue arrow, right fork*) and coactivating Munc13 proteins (data not shown).

(34). In contrast, non-exocrine secretory cells are bathed in interstitial fluid or plasma with tightly controlled Ca^{2+} concentrations. Indeed, in airway secretory cells, capacitative Ca^{2+} entry occurs exclusively at the basolateral surface that is exposed to interstitial fluid (9).

Lack of Base-line Mucin Accumulation in syt2 Null Mice—The airway secretory phenotype of *syt2* null mice, which show no spontaneous accumulation of intracellular mucin in the absence of inflammatory metaplasia but a severe defect in stimulated mucin secretion (Fig. 2), is strikingly different from that of Munc13-2 null mice, which spontaneously accumulate intracellular mucin but have only a moderate defect in stimulated mucin secretion (4). Possible explanations include differential distribution of Syt2 and Munc13-2 on distinct secretory granule populations, or intrinsic differences between Syt2 and Munc13-2 in their mechanisms of control of a single granule population. We favor the latter based upon the known physiology of Syt2 in neurons (14, 16, 17), as follows.

Fast, synchronous synaptic vesicle release occurs in close temporal and spatial proximity to the elevated cytoplasmic Ca^{2+} (~10 μM) associated with an action potential (10, 37). Slow, asynchronous release occurs after voltage-gated Ca^{2+} channels have closed and is thought to be triggered by residual elevations of cytoplasmic Ca^{2+} (~1 μM). Spontaneous release occurs at resting levels of cytoplasmic Ca^{2+} (~0.1 μM). Whereas fast, synchronous release depends upon low affinity Syts (Syt1, -2, and -9), slow, asynchronous, and spontaneous releases are instead inhibited by low affinity Syts (14, 17, 39, 40). Nonetheless, in calyx of Held neurons, synchronous (Syt2-dependent) and asynchronous (Syt2-independent) evoked releases act on the same synaptic vesicle pool (17). By analogy, we consider it most likely that Syt2 and Munc13-2 regulate a single pool of mucin granules in airway goblet cells. Furthermore, the increase in spontaneous synaptic vesicle release at neuromuscular junctions of Syt2 null mice (14) suggests that the lack of base-line mucin accumulation in these mice might reflect a similar increase in spontaneous release because of the loss of the inhibitory action of Syt2. In contrast, unactivated Munc13-2 has no inhibitory function, so its absence results only in a partial loss of secretory function at

both base-line and stimulated levels of cytoplasmic Ca^{2+}, with no apparent gain of function. Residual priming function at both Ca^{2+} levels is likely mediated by Munc13-4 that is also expressed in airway goblet cells (4, 47). This provides a parsimonious explanation of the available results, although additional experiments are required to further test this model.

Acknowledgments—We thank Wyeth for the gift of IL-13 and Christopher M. Evans for helpful discussions.

REFERENCES

1. Knowles, M. R., and Boucher, R. C. (2002) *J. Clin. Investig.* **109,** 571–577
2. Williams, O. W., Sharafkhaneh, A., Kim, V., Dickey, B. F., and Evans, C. M. (2006) *Am. J. Respir. Cell Mol. Biol.* **34,** 527–536
3. Davis, C. W., and Dickey, B. F. (2008) *Annu. Rev. Physiol.* **70,** 487–512
4. Zhu, Y., Ehre, C., Abdullah, L. H., Sheehan, J. K., Roy, M., Evans, C. M., Dickey, B. F., and Davis, C. W. (2008) *J. Physiol.* (*Lond.*) **586,** 1977–1992
5. Ehre, C., Zhu, Y., Abdullah, L. H., Olsen, J., Nakayama, K. I., Nakayama, K., Messing, R. O., and Davis, C. W. (2007) *Am. J. Physiol.* **293,** C1445–C1454
6. Rossi, A. H., Sears, P. R., and Davis, C. W. (2004) *J. Physiol.* (*Lond.*) **559,** 555–565
7. Rossi, A. H., Salmon, W. C., Chua, M., and Davis, C. W. (2007) *Am. J. Physiol.* **292,** L92–L98
8. Kemp, P. A., Sugar, R. A., and Jackson, A. D. (2004) *Am. J. Respir. Cell Mol. Biol.* **31,** 446–455
9. Bahra, P., Mesher, J., Li, S., Poll, C. T., and Danahay, H. (2004) *Br. J. Pharmacol.* **143,** 91–98
10. Chapman, E. R. (2008) *Annu. Rev. Biochem.* **77,** 615–641
11. Rizo, J., Chen, X., and Arac, D. (2006) *Trends Cell Biol.* **16,** 339–350
12. Gustavsson, N., Lao, Y., Maximov, A., Chuang, J. C., Kostromina, E., Repa, J. J., Li, C., Radda, G. K., Sudhof, T. C., and Han, W. (2008) *Proc. Natl. Acad. Sci. U. S. A.* **105,** 3992–3997
13. Maximov, A., Lao, Y., Li, H., Chen, X., Rizo, J., Sorensen, J. B., and Sudhof, T. C. (2008) *Proc. Natl. Acad. Sci. U. S. A.* **105,** 3986–3991
14. Pang, Z. P., Melicoff, E., Padgett, D., Liu, Y., Teich, A. F., Dickey, B. F., Lin, W., Adachi, R., and Sudhof, T. C. (2006) *J. Neurosci.* **26,** 13493–13504
15. Schonn, J. S., Maximov, A., Lao, Y., Sudhof, T. C., and Sorensen, J. B. (2008) *Proc. Natl. Acad. Sci. U. S. A.* **105,** 3998–4003
16. Xu, J., Mashimo, T., and Sudhof, T. C. (2007) *Neuron* **54,** 567–581
17. Sun, J., Pang, Z. P., Qin, D., Fahim, A. T., Adachi, R., and Sudhof, T. C. (2007) *Nature* **450,** 676–682
18. Fukuda, M., Kowalchyk, J. A., Zhang, X., Martin, T. F., and Mikoshiba, K. (2002) *J. Biol. Chem.* **277,** 4601–4604
19. Fukuda, M. (2004) *Biochem. J.* **380,** 875–879
20. Lynch, K. L., and Martin, T. F. (2007) *J. Cell Sci.* **120,** 617–627
21. Iezzi, M., Kouri, G., Fukuda, M., and Wollheim, C. B. (2004) *J. Cell Sci.* **117,** 3119–3127
22. Iezzi, M., Eliasson, L., Fukuda, M., and Wollheim, C. B. (2005) *FEBS Lett.* **579,** 5241–5246
23. Mohler, P. J., Davis, J. Q., Davis, L. H., Hoffman, J. A., Michaely, P., and Bennett, V. (2004) *J. Biol. Chem.* **279,** 12980–12987
24. Evans, C. M., Williams, O. W., Tuvim, M. J., Nigam, R., Mixides, G. P., Blackburn, M. R., DeMayo, F. J., Burns, A. R., Smith, C., Reynolds, S. D., Stripp, B. R., and Dickey, B. F. (2004) *Am. J. Respir. Cell Mol. Biol.* **31,** 382–394
25. Scotland, P., Zhou, D., Benveniste, H., and Bennett, V. (1998) *J. Cell Biol.* **143,** 1305–1315
26. Kirkham, S., Sheehan, J. K., Knight, D., Richardson, P. S., and Thornton, D. J. (2002) *Biochem. J.* **361,** 537–546
27. Mohler, P. J., Schott, J. J., Gramolini, A. O., Dilly, K. W., Guatimosim, S., duBell, W. H., Song, L. S., Haurogne, K., Kyndt, F., Ali, M. E., Rogers, T. B., Lederer, W. J., Escande, D., Le Marec, H., and Bennett, V. (2003) *Nature* **421,** 634–639
28. Li, H., Cho, S. N., Evans, C. M., Dickey, B. F., Jeong, J. W., and DeMayo, F. J. (2008) *Genesis* **46,** 300–307
29. Nguyen, L. P., Omoluabi, O., Parra, S., Frieske, J. M., Clement, C., Ammar-Aouchiche, Z., Ho, S. B., Ehre, C., Kesimer, M., Knoll, B. J., Tuvim, M. J., Dickey, B. F., and Bond, R. A. (2008) *Am. J. Respir. Cell Mol. Biol.* **38,** 256–262
30. Evans, C. M., Kim, K., Tuvim, M. J., and Dickey, B. F. (2009) *Curr. Opin. Pulm. Med.* **15,** 4–11
31. Sheehan, J. K., Kirkham, S., Howard, M., Woodman, P., Kutay, S., Brazeau, C., Buckley, J., and Thornton, D. J. (2004) *J. Biol. Chem.* **279,** 15698–15705
32. Dellis, O., Dedos, S. G., Tovey, S. C., Taufiq, U. R., Dubel, S. J., and Taylor, C. W. (2006) *Science* **313,** 229–233
33. Petersen, O. H., and Tepikin, A. V. (2008) *Annu. Rev. Physiol.* **70,** 273–299
34. Nguyen, T., Chin, W. C., and Verdugo, P. (1998) *Nature* **395,** 908–912
35. Davis, C. W., Dowell, M. L., Lethem, M., and Van Scott, M. (1992) *Am. J. Physiol.* **262,** C1313–C1323
36. Danahay, H., Atherton, H. C., Jackson, A. D., Kreindler, J. L., Poll, C. T., and Bridges, R. J. (2006) *Am. J. Physiol.* **290,** L558–L569
37. Heidelberger, R. (2007) *Nature* **450,** 623–625
38. Zhang, B., Koh, Y. H., Beckstead, R. B., Budnik, V., Ganetzky, B., and Bellen, H. J. (1998) *Neuron* **21,** 1465–1475
39. Chicka, M. C., Hui, E., Liu, H., and Chapman, E. R. (2008) *Nat. Struct. Mol. Biol.* **15,** 827–835
40. Littleton, J. T., Stern, M., Perin, M., and Bellen, H. J. (1994) *Proc. Natl. Acad. Sci. U. S. A.* **91,** 10888–10892
41. Nagy, G., Kim, J. H., Pang, Z. P., Matti, U., Rettig, J., Sudhof, T. C., and Sorensen, J. B. (2006) *J. Neurosci.* **26,** 632–643
42. Perez-Vilar, J., Ribeiro, C. M., Salmon, W. C., Mabolo, R., and Boucher, R. C. (2005) *J. Histochem. Cytochem.* **53,** 1305–1309
43. Ribeiro, C. M., Paradiso, A. M., Livraghi, A., and Boucher, R. C. (2003) *J. Gen. Physiol.* **122,** 377–387
44. de Brito, O. M., and Scorrano, L. (2008) *Nature* **456,** 605–610
45. Widdicombe, J. G. (1989) *Eur. Respir. J.* **2,** 107–115
46. Effros, R. M., Peterson, B., Casaburi, R., Su, J., Dunning, M., Torday, J., Biller, J., and Shaker, R. (2005) *J. Appl. Physiol.* **99,** 1286–1292
47. Koch, H., Hofmann, K., and Brose, N. (2000) *Biochem. J.* **349,** 247–253